ACS OMEGA

Open Access

http://pubs.acs.org/journal/acsodf

Article

Hydrates of N-((10-Chloroanthracen-9-yl)methyl)-3-(1H-imidazol-1-yl)propan-1-ammonium Cobalt(II), Copper(II), and Zinc(II) 2,6-Pyridinedicarboxylate: Reversible Crystallization

Abhay Pratap Singh and Jubaraj B. Baruah*

Cite This: *ACS Omega* 2024, 9, 47848−47856

Read Online

ACCESS | Metrics & More | Article Recommendations | Supporting Information

ABSTRACT: In a quest to explore interconvertible assemblies of hydrates of cobalt(II), copper(II), and zinc(II) 2,6-pyridinedicarboxylate (**26-pdc**), complexes having cation of a chloro-substituted analogue N-{(10-chloroanthracen-9-yl)methyl}-3-(1H-imidazol-1-yl)propan-1-amine were investigated. In the case of cobalt and copper complexes, a crystallized stable hydrate and a less stable methanol hydrate were guided by concentration-dependent crystallizations. The unit-cells of the crystals of the methanol hydrates of the two cobalt and copper complexes each belong to the $P\bar{1}$ space group but have different stoichiometries as well as large differences in packing. These hydrates could be reversibly crystallized in a predictable manner. The unit-cell volumes of the methanol hydrate of the cobalt complex were four-times smaller than that of the respective stable form ($C2/c$ space group), whereas similar hydrates of the copper complex had a two-times smaller unit-cell volume than that of the stable form. The cations of the stable forms assembled together and formed zigzag ladder-like chains. The spaces present in between the assembled chains were filled with clusters of face to face stacked anions. The transformation to stable form required a bottom-up building process of the unit-cell starting from a smaller unit-cell of the less stable hydrates. Fluorescence spectroscopic studies showed the possibility of two forms of assemblies of the zinc-complex in solution, but crystallization had yielded only the stable form.

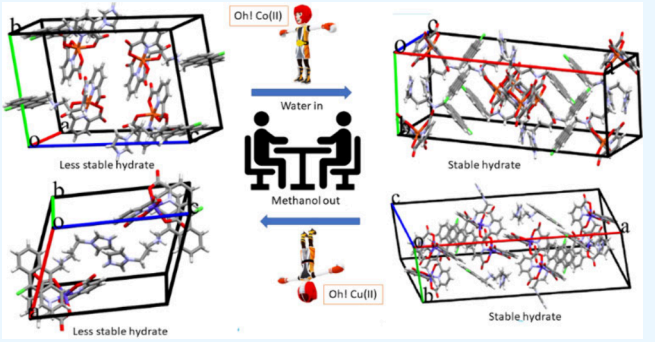

INTRODUCTION

The role of water in the microscopic and macroscopic world is indispensable for everyday activities and there are many to enjoy by a beginner developed through interesting experiments.[1−3] The same process is used and also understanding gets complicated while dealing at the molecular level.[4−6] Water molecules of crystallization contribute to emission,[7−12] magnetic properties,[13−18] proton conductors,[19−23] and energy storage.[24] The water molecules in gas-clathrates[25,26] have industrial values and influence the efficacy of drugs.[27,28] The water molecules associated with anions,[29−31] ion channels,[32] have their own applications. Water crystallization of inorganics also has importance in gels,[33,34] various hydrates, and aqua complexes. It may be noted that there are examples such as polymorphs formed through crystal group transformation (monoclinic to triclinic) that differ in the number of symmetry nonequivalent molecules in the unit-cell having large differences in morphology.[35] Reversible polymorphic transformation of hydrates and phase transformations are reported in the literature.[36,37] Solvents playing key roles in an interconversion of polymorphic forms and dictating the stability of metastable forms are well-known.[38−41] Solvent-guided synthesis of the optically active coordination complex[42] and reversible bindings of solvent with metal organic frameworks[43] provide interest in the role of any solvent molecules in solution to generate materials with specific properties. Water molecules stored within self-assembled containers have scopes in harvesting water from the atmosphere,[43] modulation of evaporation, and use for improving properties.[44] Furthermore, hydrates of pharmaceutical compounds involve high-level of complexities in isolating and retaining crystalline forms.[45] Braun and coworkers explained some of the challenges by bringing classical examples of hydrates of drug molecules to show the numbers of hydrates and their interconversions.[46,47] In our previous studies, we found that concentration-dependent crystallizations of different metal complexes with the same set of ligands resulted in different hydrates. Among those, the metastable hydrates could also be structurally characterized.[48,49] On the other hand, the polymorphic cocrystals can

Received: September 26, 2024
Revised: October 21, 2024
Accepted: November 5, 2024
Published: November 19, 2024

https://doi.org/10.1021/acsomega.4c08822
ACS Omega 2024, 9, 47848−47856

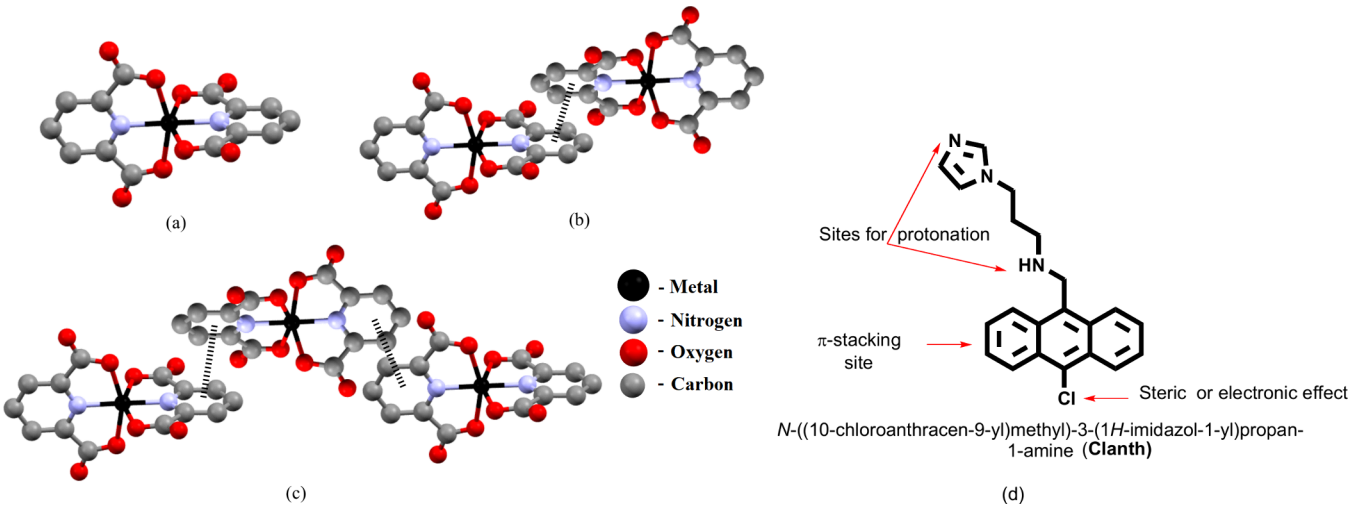

Figure 1. (a)−(c) The stacking among metal 2,6-pyridinedicarboxylates (Drawn with Chem Draw Ultra 3D). (d) The precursor (**Clanth**) of the cationic counterparts of the complexes.

be distinguished by spectroscopic means[50] other than crystallography as a tool. Depending on the solvent of crystallization, different assemblies were formed; hence, dislodging such assemblies and regaining the original form will provide a larger perspective to prepare soft materials.[51−53] In our research endeavor, different stacking arrangements among chelate rings in different hydrates of chelated metal-2,6-pyridinedicraboxylate in different hydrates have provided a simple building unit to explore with various possibilities through variation of central metal ions and decoration of the core anions with organic cations with versatile properties. Such facts were reflected in various hydrates that could be prepared by changing crystallization conditions, as hydrates having discrete units of such anions (Figure 1a) in respective self-assembly were least stable, whereas the ones having dimer-like (Figure 1b) or polymer-like arrangements (Figure 1c) of stacked anions in assemblies had higher stabilities. With such information in hand, we shifted our attention to study hydrates from bivalent cobalt, copper, and zinc 2,6-pyridine-dicarboxylate (**26-pdc**) complexes having the cation of a chloro-substituted analogue, N-{(10-chloroanthracen-9-yl)-methyl}-3-(1H-imidazol-1-yl)propan-1-amine (abbreviated as **Clanth**, Figure 1). Primarily, each member of the class of the above compound would have a fluorescent anthracenyl unit attached through a flexible part. An ionic assembly of them has the scope to modulate emission, which may in turn be used as a probe to study recognition and interconversions. Hence, the study of such assemblies of ionic cocrystals and hydrates has high potential as observed with hydrates in batteries,[54] solar-cells,[55] and in high-energy compounds such as explosives.[56] **Clanth** was chosen to limit and provide packing constraints to have limited numbers of hydrates through the constraints of weak interactions and the steric effect of the chlorine atom in the molecule. This was in anticipation of cooperative interactions such as C−H···Cl, or Cl···X (heteroatom) interactions, or the changes in assembling due chlorine atom of the cation. These would change the assembling property of the cations from the unsubstituted one. On the other hand, adequately arranged relatively larger organocations with anions of inorganic complex in a lattice would provide better interstitial spaces than conventional assemblies of small ions to modulate hydrations or guest recognitions. As a part of wider prospects of ionic assemblies of inorganic complexes, characterizations and reversible transformations of different hydrates are described in this manuscript.

EXPERIMENTAL SECTION

General. Infrared spectra of the solid samples were recorded on a PerkinElmer Spectrum-Two FT-IR spectrophotometer in the region 4000−400 cm^{-1} using attenuated total reflectance method. The ^1H NMR spectra were recorded on a BRUKER Ascend-600 MHz NMR spectrometer using TMS as the internal standard. Microscopic images of crystal morphologies were recorded on a Carl Zeiss Gemini 300 FESEM instrument by a drop-casting method. The thermogravimetric analyses were done on a PerkinElmer TGA 4000, under nitrogen gas flow. Fluorescence emission spectra in solution were recorded on a Horiba Jobin Yvon Fluoromax-4 spectrofluorometer. Dynamic light scattering studies were performed using Malvern Zetasizer Nano ZS90. The solvent used were from Merck, EMPLURA grades.

Clanth was prepared by reductive amination of 10-chloro-9-anthraldehyde with 1-(3-aminopropyl)imidazole in the presence of $NaBH_4$ in methanol by following a procedure similar to the reported procedure with analogous compound[57] (Isolated yield 62%). ^1H NMR (600 MHz, DMSO-d_6): 8.50 (d, J = 6 Hz, 2H), 8.47 (d, J = 6 Hz, 2H), 7.71 (t, J = 6 Hz, 2H), 7.66 (t, J = 6 Hz, 2H), 7.53 (s, 1H), 7.07 (s, 1H), 6.84 (s, 1H), 4.60 (s, 2H), 3.99 (t, J = 6 Hz, 2H), 2.69 (t, J = 6 Hz, 2H), 1.89 (p, J = 6 Hz, 2H). ESI-MS: m/z $[M + H]^+$: 350.1414. IR (neat, cm^{-1}): 3236 (s), 2943 (m), 2838 (m), 1622 (w), 1551 (w), 1503 (s), 1439 (s), 1363 (m), 1328 (s), 1280 (m), 1259 (m), 1225 (s), 1172 (w), 1112 (s), 1075 (s), 1033 (s), 927 (s), 862 (w), 839 (w), 818 (s), 795 (m), 751 (s), 740 (s), 731 (s), 663 (s), 651 (s). ESI mass found (m/z): 350.1346 (calcd M^+ + H) found 350.1414.

Crystallization of the Hydrates. The crystals of the hydrates were obtained from similar crystallization procedures by varying the concentrations of the components in a solution fixed volume of solvent. The typical procedure for crystallization of **Zn−H_2Clanth** is given below. The procedures for crystallization of the other hydrates were similar, which are listed in Table 1.

https://doi.org/10.1021/acsomega.4c08822
ACS Omega 2024, 9, 47848−47856

Table 1. Crystallization Conditions for Preparation of the Hydrates

Hydrate[a]	$M(OAc)_2 \cdot xH_2O$[@] (mmol)	2,6-H_2pdc (mmol)	Clanth (mmol)	Time for crystallization
Co−H_2Clanth-Int	0.2	0.4	0.2	2 days
Co−H_2Clanth[b]	0.4	0.8	0.4	3−4 days
Cu−H_2Clanth-Int	0.2	0.4	0.2	2 days
Cu−H_2Clanth[b]	0.4	0.8	0.4	3−4 days
Zn−H_2Clanth[b]	0.4	0.8	0.4	3−4 days

[a]In each case, 20 mL of methanol was taken; M = Zn, x = 2, M = Cu, x = 1 and M = Co, x = 4. [b]= 2 mL of water was added after 12 h to dissolve a precipitate formed and allowed to recrystallize.

Zn−H_2Clanth. A powdered solid sample of **Clanth** (140 mg, 0.40 mmol) was added to a well stirred solution of 2,6-pyridinedicarboxylic acid (134 mg, 0.80 mmol) and zinc(II) acetate dihydrate (88 mg, 0.40 mmol) in methanol (20 mL). The resulting solution was stirred for about 12 h, and 2 mL of water was added to dissolve the appeared precipitate; after that it was kept undisturbed for crystallization, providing the crystals of **Zn−H_2Clanth**. Yield of the crystals: **Zn−H_2Clanth** (297 mg; 83%); **Co−H_2Clanth** (167 mg; 45%); **Cu−H_2Clanth** (163 mg; 46%). The exact yield of the two intermediate solvates could not be ascertained as they transformed once taken out from solution.

Crystal Structures Determination. The diffraction data for the hydrates were collected by using a Bruker APEX-II CCD diffractometer at room temperature for all of the crystals. The refinement of and cell reductions were carried out using SAINT and XPREP software. Structures were solved by direct methods using SHELXS-97 and were refined by full-matrix least-squares on F^2 using SHELXL-14 and OLEX2 programs. All non-hydrogen atoms were refined in anisotropic approximation against F^2 of all reflections. Hydrogen atoms were placed at their geometric positions by riding and were refined in an isotropic approximation. The crystallographic information file of **Cu−H_2Clanth-Int** showed B-alert, as we could not locate the hydrogen atom of water due to diffraction quality and instability. The crystal and refinement parameters are listed in Table 2.

RESULTS AND DISCUSSIONS

Clanth was characterized by NMR, IR, and mass spectroscopy, and its crystal structure was also determined (Figure 2a). The geometry adopted by the flexible $-(CH_2)_3NH(CH_2)-$ part guided the orientations of the imidazole and chloroanthracenyl units. The angle between the planes of these two units was 81.80° (Figure 2b), showing crystallization from the reactions between **Clanth** with 2,6-pyridinedicarboxylic acid in the presence of metal(II) acetates of cobalt, copper, or zinc, which resulted in the crystallization of hydrates of them to

Table 2. Crystal and Refinement Parameters of the Compounds

Parameters	Clanth	Zn−H_2Clanth	Cu−H_2Clanth-Int	Cu−H_2Clanth	Co−H_2Clanth-Int	Co−H_2Clanth
Formula	$C_{21}H_{20}ClN_3$	$C_{35}H_{28}ClN_5O_8Zn$ [+ solvent]	$C_{73}H_{72}Cl_2N_{10}O_{21}Cu_2$	$C_{35}H_{28}ClN_5O_8Cu$ [+ solvent]	$C_{36}H_{34}ClN_5O_{10}Co$	$C_{35}H_{34}ClN_5O_{11}Co$ [+ solvent]
CCDC No.	2385089	2363164	2363162	2363163	2363160	2363161
Mol.wt.	349.85	747.44	1623.38	745.61	791.06	795.05
Crystal System	triclinic	monoclinic	triclinic	Monoclinic	triclinic	monoclinic
Space group	$P\bar{1}$	*C*2/*c*	$P\bar{1}$	*C*2/*c*	$P\bar{1}$	*C*2/*c*
a (Å)	8.256(5)	40.142(3)	10.591(12)	40.23(2)	10.881(14)	40.171(4)
b (Å)	8.510(5)	11.730(8)	14.981(17)	11.745(7)	10.909(14)	11.694(11)
c (Å)	13.138(8)	16.302(11)	22.983(3)	16.106 (10)	15.370(2)	16.270(16)
α (deg)	86.269(2)	90	92.633(3)	90	92.594(5)	90
β (deg)	72.619(2)	111.643(2)	92.562(3)	111.810(17)	110.565(3)	111.556(3)
γ (deg)	85.562(2)	90	93.924(3)	90	91.135(4)	90
V (Å^3)	877.5(9)	7135.3(8)	3630.5(7)	7065(7)	1705.1(4)	7108.7(12)
Z	2	8	2	8	2	8
Density, g cm^{-3}	1.324	1.392	1.485	1.402	1.541	1.486
Abs. coeff., mm^{-1}	0.226	0.820	0.743	0.751	0.651	0.627
F (000)	368	3072	1680	3064	818	3288
Total no. of reflections	3301	7863	17273	6218	6919	7809
Reflections, I > 2σ(I)	2859	5966	12104	4844	5588	5761
Max. θ/°	25.681	25.242	25.242	25.000	25.242	25.242
Ranges (h, k, l)	$-10 \le h \le 10$	$-51 \le h \le 51$	$-13 \le h \le 13$	$-47 \le h \le 47$	$-13 \le h \le 13$	$-51 \le h \le 51$
	$-10 \le k \le 10$	$-15 \le k \le 15$	$-19 \le k \le 19$	$-13 \le k \le 13$	$-13 \le k \le 13$	$-14 \le k \le 14$
	$-16 \le l \le 16$	$-20 \le l \le 20$	$-30 \le l \le 30$	$-19 \le l \le 19$	$-19 \le l \le 19$	$-20 \le l \le 20$
Complete to 2θ (%)	99.3	99.9	99.8	99.9	99.5	99.7
Data/restraints/parameters	3301/0/230	7863/0/455	17273/0/984	6218/0/455	6919/0/487	7809/0/483
GooF (F^2)	0.935	1.151	1.127	1.095	1.174	1.056
R indices [I > 2σ(I)]	0.0666	0.0601	0.0673	0.0428	0.0680	0.0645
wR_2 [I > 2σ(I)]	0.1732	0.1094	0.1308	0.0985	0.1145	0.1821
R indices (all data)	0.0764	0.0839	0.1051	0.0621	0.0887	0.0894
wR_2 (all data)	0.1835	0.1214	0.1504	0.1148	0.1230	0.2144

https://doi.org/10.1021/acsomega.4c08822
ACS Omega 2024, 9, 47848−47856

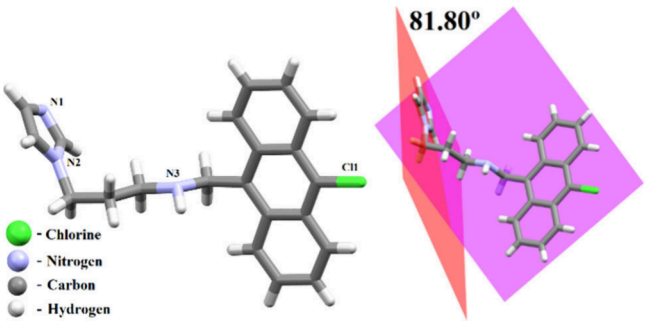

Figure 2. (a) The crystal structure of **Clanth** and (b) the angle between the planes containing the chloro-anthracenyl and imidazole parts of **Clanth**.

have nearly perpendicular orientation with respect to each other. The concentration-dependent corresponding 2,6-pyridinedirboxylate complexes are listed in Figure 3. During

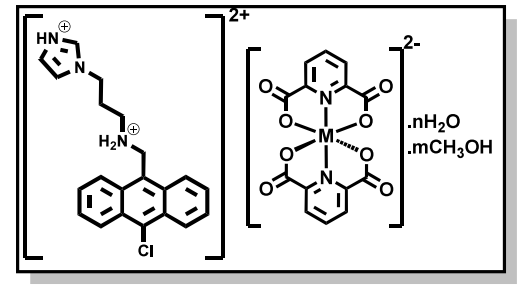

Zn-H_2Clanth, n = 4, m = 0, (Monoclinic C2/c, V = 7135.3 Å^3)
Co-H_2Clanth, n = 5, m = 0, (Monoclinic C2/c, V = 7108.7 Å^3)
Cu-H_2Clanth, n = 4, m = 0, (Monoclinic C2/c, V = 7065.0 Å^3)
Co-H_2Clanth-Int, n = 1, m = 1 (Triclinic P-1, V = 1705.1 Å^3)
Cu-H_2Clanth-Int, n = 1, m = 1.5 (Triclinic P-1, V = 3630.5 Å^3)

Figure 3. Hydrates of the cobalt, copper, and zinc-26-pdc complexes having **H_2Clanth** cation.

the course of complex formation, **Clanth** was protonated at −NH− and one of the nitrogen atoms of the imidazole by the in situ abstraction of protons from the carboxylic acid groups of $H_2$26-pdc. Accordingly, each complex/hydrate had **H_2Clanth** dication as the cationic part. In general, diprotonation of such ligands is easily caused by a carboxylic acid.[58] In contrast to our earlier finding on observing three types of hydrates,[48,49] in the present study, only two types of hydrates were observed of the copper or cobalt complex. However, only the stable form of the hydrate of the zinc complex was observed. The crystals of all the stable hydrates included in the Figure 3 were monoclinic, belonging to the $C2/c$ space group. The crystals of stable hydrates were obtained when the reaction was performed at a relatively higher concentration as listed in Table 1. All the stable hydrates were prepared by recrystallization of a precipitate formed during the reaction, which was dissolved in water and then allowed to crystallize. The stable hydrates obtained for the copper and zinc complexes were tetrahydrate, whereas the stable form of the hydrate of the cobalt complex had five water crystallization molecules (Figure 3). The unit-cell volumes of the single crystals of the stable hydrates followed an order zinc-complex > cobalt-complex > copper-complex. This trend was not found as per the order of the ionic radius, Zn(II) > Cu(II) > Co(II). It was due to the fact that the cobalt complex was a penta-hydrate and the other two were tetrahydrate. On the other hand, both less stable crystals of hydrate (alternatively, mixed solvate) belonged to triclinic, $P\bar{1}$ space group. The two less-stable hydrates had different amounts of water with respect to methanol molecules of crystallization.

The ratio of water to methanol in the less stable hydrate of the cobalt complex was 1:1, whereas the similar less stable hydrate of the copper complex had a ratio 1:1.5. In the case of cations without a substituent,[48,49] the less stable form of hydrate had a water−methanol ratio 1:1.5. Among the three stable hydrates of the series, each had close similarity in respective structure, hence, only a representative structure of the cobalt(II) complex Co−H_2**Clanth** is shown in Figure 4a. The self-assembly of it contained two $[Co(26\text{-pdc})_2]^{2-}$ in close vicinity that remained as pairs. These anions located at parallel position were not eclipsing each other but located at translated positions. Each pair was stabilized by $N-H_{(ammonium)}\cdots O_{(carbonyl)}$ and $N-H_{(ammonium)}\cdots O_{(carboxylate)}$ interactions and also by the two water molecules of the hydrate holding the same pair at the other side (Figure 4a). It is well established that chelate−chelate stacking interactions contribute to the stability of assemblies.[59] The stacking interactions among coordinated pyridine rings in the metal complex vary from 7 to 33 kcal/mol, and stacking among two free pyridine rings provides a stability of ∼4 kcal/mol. However, a metal−pyridine bond provides stability of about 7 kcal/mol.[60] Hence, the coordinated pyridine of the 26-pdc and the stacking among the pyridine rings contributed to the stability of assemblies in the hydrates. There are also instances where other factors such as hydrogen bonds may be the prime factor over the stacking interaction.[61] In the present case, $^+$N−H was involved in charge-assisted hydrogen bonds. The interactions of water molecules with two anions from one side and the $^+$N−H from the other side held two anions together as a pair. Here, the apparent portion formed by weak interactions to hold two

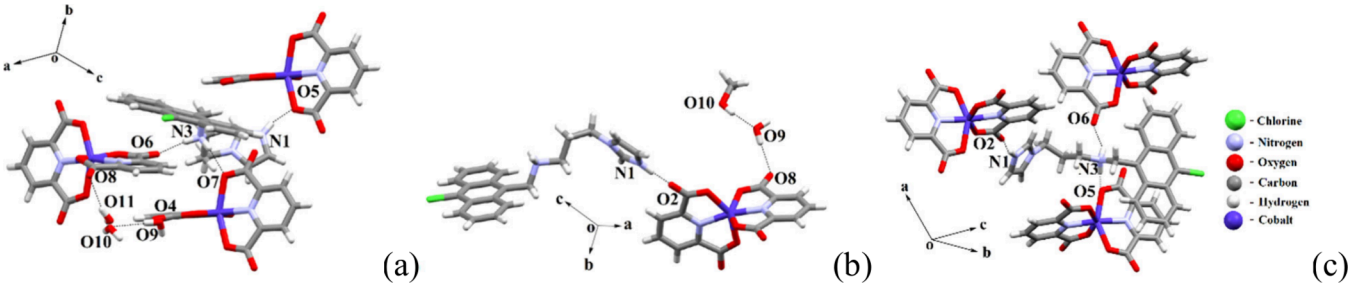

Figure 4. (a) Self-assembly of **Co−H_2Clanth** showing two rings of the anions eclipsing each other to have stacking interaction. (b) The crystal structure of **Co−H_2Clanth-Int**. (c) The hydrogen bonded assemblies of **Co−H_2Clanth-Int** showing hydrogen bond between the ions.

https://doi.org/10.1021/acsomega.4c08822
ACS Omega 2024, 9, 47848−47856

anions at the closest vicinity shown in Figure 4a has a chloro-anthracenyl unit that is stacked with a plane of 26-pdc chelate. The distance between the centroids of the chloro-anthracenyl plane to the chelated 26-pdc-ring was 3.990 Å and hence showed stacking interactions between these sets of rings. Thus, the higher stability of the hydrate was due to the hydrogen bonds holding the chelated anions in pairs and the stacking of chelate ring with the anthracenyl ring, as illustrated in Figure 4a. The **H_2Clanth** cation was directly linked to the anions through hydrogen bonds in **Co−H_2Clanth-Int** (Figure 4b).

These were linked by $^{+}$N1−$H_{imidazole}$···$O2_{carbonyl}$ {d_D···$_A$, 2.629(5)Å, < D-H···A 166.0(6)°}, N3−$H_{ammonium}$···$O6_{carbonyl}$ {d_D···$_A$, 2.797(4)Å, < D-H···A 144°}, and N3−$H_{ammonium}$···$O5_{carboxylate}${d_D···$_A$, 2.807(4)Å, < D-H···A 159°} hydrogen bonds (Figure 4c). However, the methanol molecule acted as hydrogen bond donor to the oxygen atom (O9) of water {O10−H···O9; d_D···$_A$, 2.751(7)Å, < D-H···A 172°} and the same water molecule was hydrogen bonded to the carbonyl of an oxygen atom by {O9−H···O8, d_D···$_A$, 2.964(5)Å, < D-H···A 173°}. This terminated a hydrogen bonded chain, and the methanol and water remained in the interstices with the support of ions. However, in the self-assembly of the **Co−H_2Clanth**, the cation was linked by $^{+}$N1−$H_{imidazole}$···$O5_{carboxylate}$ {d_D···$_A$, 2.811(4)Å, < D-H···A 158°}, N3−$H_{ammonium}$···$O7_{carboxylate}$ {d_D···$_A$, 2.808(4)Å, < D-H···A 165°}, and N3−$H_{ammonium}$···$O6_{carbonyl}${d_D···$_A$, 2.778(4)Å, < D-H···A 167°} interactions (Figure 4a). A water molecule was held by hydrogen bonding to oxygen atom of another water molecule {O9−H···O10; d_D···$_A$, 2.942(6)Å, < D-H···A 166°} and {O10−H···O11; d_D···$_A$, 2.872(6)Å, < D-H···A 162(8)°}. The water molecule having O11 was hydrogen bonded to the carbonyl oxygen atom by {O10−H···O8, d_D···$_A$, 2.929(4)Å, < D-H···A 149(6)°}. Thus, in this case, the $-^{+}NH_2-$ as well as the hydrogen bonds of cation with anion and that of water molecules with anion provided the necessary linkages to have a stable structure.

The crystal structure of **Cu−H_2Clanth-Int** showed that the cation of the complex was hydrogen bonded to water by $^{+}$N4−$H_{imidazole}$···$O21_{water}$ {d_D···$_A$, 2.662(6)Å, < D-H···A 171.0°} and $^{+}$N1−$H_{imidazole}$···$O20_{water}$ {d_D···$_A$, 2.765(5)Å, < D-H···A 165.0(4)°} interactions. It was also hydrogen bonded to the anions through an intervening water molecule {O20−H···$O10_{carbonyl}$; d_D···$_A$, 2.755(4)Å, < D-H···A 163°}. One methanol and two water molecules of crystallization formed a hydrogen bonded chain holding two independent anions at two ends {O19−H···$O5_{carboxylate}$; d_D···$_A$, 2.668(6)Å, < D-H···A 175°} and {O21−H···O19; d_D···$_A$, 2.700(8)Å, < D-H···A 172°; O21−H···O20; d_D···$_A$, 2.758(6)Å, < D-H···A 144°} (Figure 5a). This showed that the packing patterns of the two less stable hydrates had large differences in the solvent acting as intervening molecules between two anions at extreme ends. In the case of cobalt, the methanol−water hydrogen bond was terminated, but in the case of the less stable hydrate of copper, it was a hydrogen bonded chain of anion···water···water···methanol···anion. There was a large difference in the unit-cell volume of the crystals of the two less stable hydrates. The unit cell of **Co−H_2Clanth-Int** was 1705 (4) Å^3, this was one-fourth of the unit cell of the stable hydrate. However, **Cu−H_2Clanth-Int** had unit-cell volume of 3630.5(7) Å^3, which was approximately double the volume of the cobalt counterpart **Co−H_2Clanth-Int**. The difference in the unit-cell volume was indeed not reflected in the number of molecules per unit cell; the Z value of the crystals of the less stable hydrates was 2 in

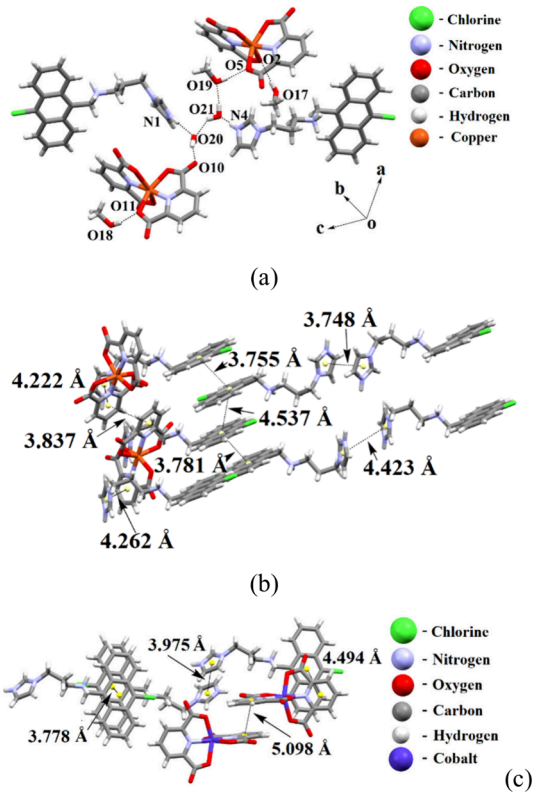

Figure 5. (a) The hydrogen bonded assembly of **Cu−H_2Clanth-Int**. Stacking among the rings in self-assembly of (b) **Cu−H_2Clanth-Int**, (c) **Co−H_2Clanth-Int**.

each case. The analysis of the stacking patterns in each case showed that their structures also had differences in the stacking arrangements among the anions. Both had stacking of chelates, but the hydrate of the cobalt complex was larger (5.098 Å) than the one observed in the hydrate of copper complex (3.755−4.537 Å) as shown in Figure 5(b) and (c). The three stable hydrates (Co, Cu, Zn complexes) possessed assembled dimers of anions in their respective lattices. These dimers were held together by bridging water molecules and the $-NH_2^{+}-$ part of the cation. On the other hand, the unstable hydrate of the cobalt complex had stacked dimers of anions, which were formed by eclipsing chelate rings with a distance of separation of 5.098 Å, while the unstable hydrate of the copper complex had layers of anions having stacking among each other. In such a case, the centroid to centroid distance between the planes of the two eclipsing chelating ligands was 3.837 Å. As the hydrates had extensive stacking interactions, the interactions among same type of planar units or two different types of planar units were sorted from self-assemblies and listed in Table S6. The nature of the stacking between the rings varied among different hydrates. The intermolecular stacking interactions between chloro-anthracene rings and also between the 26-pdc rings dominated the packings of the stable forms of the hydrates. However, the intermediate cobalt hydrate had stacking among anions, but the distance between the eclipsing portions was 5.098 Å. This showed very weak interactions between them. However, the distance of separation of chloro-anthracenyl·26-pdc stack in the assembly of it was 4.494 Å. The less stable hydrate of the copper complex had stacks among the chloro-anthracenyl ring with the chloro-anthracenyl ring or imidazolium with the imidazolium unit. The latter

https://doi.org/10.1021/acsomega.4c08822
ACS Omega 2024, 9, 47848−47856

being a repulsive interaction, the structure underwent facile changes by solvent−solute interactions. The presence of such repelling stacks helped it to convert to a stable form. This reversible conversion increased the versatility for studying the transformations similar to the one suggested in other hydrate systems.[46,47,54] The less stable hydrate of the cobalt complex had anions and cations located at alternate positions providing 1D-linear arrangements. The solvent molecules were located between the layers formed by assembled arrangements of those 1D-arrangements (Figure S14). However, the less stable hydrate of the copper complex had a Lamellar-like structure. In the packing, chloro-anthracenyl units were projecting in one direction, and the chains were arranged such that chloro-anthracenyl units of two chains at immediate neighborhood were eclipsed (viewed along *ab*-crystallographic plane). The two chains had stacking interactions. The solvent molecules were located between the sides of the chain on the side having the hydrophilic part as shown in Figure S16. Three stable hydrates had similar zigzag ladder-like arrangements from the arrangements of the cations. The self-assembling of the ladder-like arrangements provided spaces to accommodate two pairs of stacked anions in each void (Figures S15, S17, and S18).

The phase-purities of all the three stable hydrates were confirmed by recording powder XRD patterns of the respective samples and comparing them with the simulated ones. The amounts of water present in the hydrates were reflected in the respective weight loss at the 40−100° in the thermogravimetry illustrated in Figures S9−S11. From the field emission scanning electron microscopy (FESEM) of the less stable cobalt hydrate as well as the stable form, we found that the less stable form had nanofibrous crystals (Figure 6) with about 200

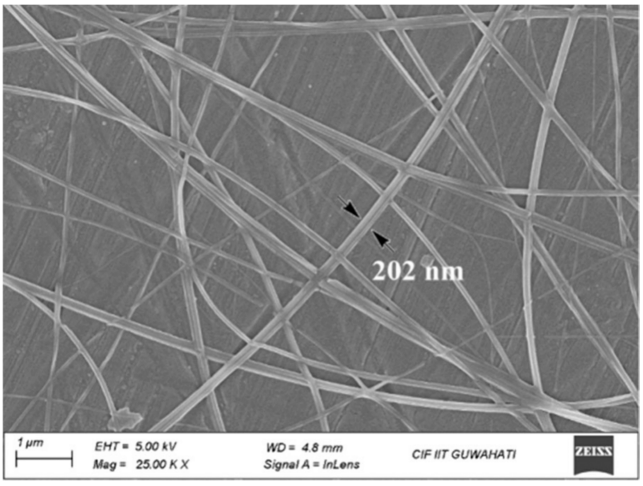

Figure 6. FESEM image of **Co−H_2Clanth-Int**.

nm width, and the stable form provided flakes of mesoscopic size (Figure S6(a)). The image revealed that the stable hydrate of the copper complex had micron-sized rod-shaped crystals, which were about 2.6 μM × 54.0 μM in size (Figure S6(b)). The SEM image of the lesser stable hydrate of the copper complex was not possible due to immediate transformation during drop-casting. The only form of zinc observed had a dense cross-linked nanofibrous structure with breadth of about 182 nm (Figure S6(c)).

The two forms of hydrates of the cobalt or copper complexes underwent reversible transformation upon changing recrystallization conditions. For example, the freshly prepared crystals of the intermediate mixed hydrates automatically got converted upon contact with moisture or water to provide the stable hydrates; alternatively, the crystals of stable hydrate, upon dissolution in the solvent from a concentration at which the intermediate was originally crystallized, yielded the crystals of the less stable form. This was an interesting point as the stoichiometry of the less stable form with respect to a stable form was not identical, nor were the Z values. Namely, the less stable form of the cobalt complex had unit-cell volume 1705.1 (4) Å^3 (space group $P\bar{1}$, Z = 2), whereas the stable form had unit-cell volume 7108.7 (12) Å^3 (space group $C2/c$, Z = 8); thus, for such a transformation, there must be an increase in unit-cell volume (approx. 4-times) by changing in the numbers of molecules per unit cell (Z value). However, the analogous copper hydrates less stable form had 3630.5(7) Å^3 (Space group $P\bar{1}$, Z = 2) and stable form had 7065(7) Å^3 (space group ($C2/c$, Z = 8), approximately double the volume of the less stable form. In each case, there was a requirement of extra water molecules replaced by methanol or vice versa. From the point of internal structural changes, it may be viewed as a change in the domain of the less stable cobalt complex to the new domain of the stable form with an increment of four-fold (Figure 7a). However, the less stable hydrate of the copper complex underwent doubling of the unit-cell volume to generate the unit-cell of the stable form (Figure 7b). Alternately, the stacking among the rings in different forms had to be reconstructed in each transformation, and it happened through the competitive effects of water and methanol to remain in the assembly within a unit cell. It has been reported in literature that the exchange of water and methanol molecule affects the unit-cell surface differently depending on the functional groups.[38] The present sets of hydrates differ from reported hydrates of similar compounds as the transformations between space groups and reversibility in transformation were different from similar systems where there were no chloride substituents. Our earlier published examples had no chloro-substituent, and three different types of hydrates in each case was observed; instead, we have here two types of hydrates. In the present case, the space group transformation caused 2-fold or 4-fold change in unit-cell volume. The transformation between the $C2/c$ space-group and **$P\bar{1}$** space-group requires minimum symmetry changes. The transformations between these space groups were found in pressure-induced crystal to crystal transformations.[61,62] For example, pressure-induced polymorphic transition of ferrous sulfate displacement of sulfate anions as well as FeO_6 units occurred.[63] In the case of the zinc complex, only the tetra-hydrate was crystallized, and many attempts to crystallize another form of hydrate were not successful. But, we could clearly observe with the naked eye the intermediate form transforming like a vanishing form from the solution and could not be isolated and characterized. So, we took advantage of the fluorescent nature of the cationic part to find out if any feature of the intermittent species could be observed during the transformation. It showed that a solution prepared at the concentration at which an unstable form would have formed (based on other analogues with cobalt and copper) showed an emission peak at 428 nm. This corresponded to the stable form of the hydrate from independent experiment with the stable form (Figure S19). This emission peak was split, showing two peaks at 425 and 431 nm upon the addition of water (Figure 8). The emissions at these wavelengths were increased as amounts of water increased. This showed that in the case of

https://doi.org/10.1021/acsomega.4c08822
ACS Omega 2024, 9, 47848−47856

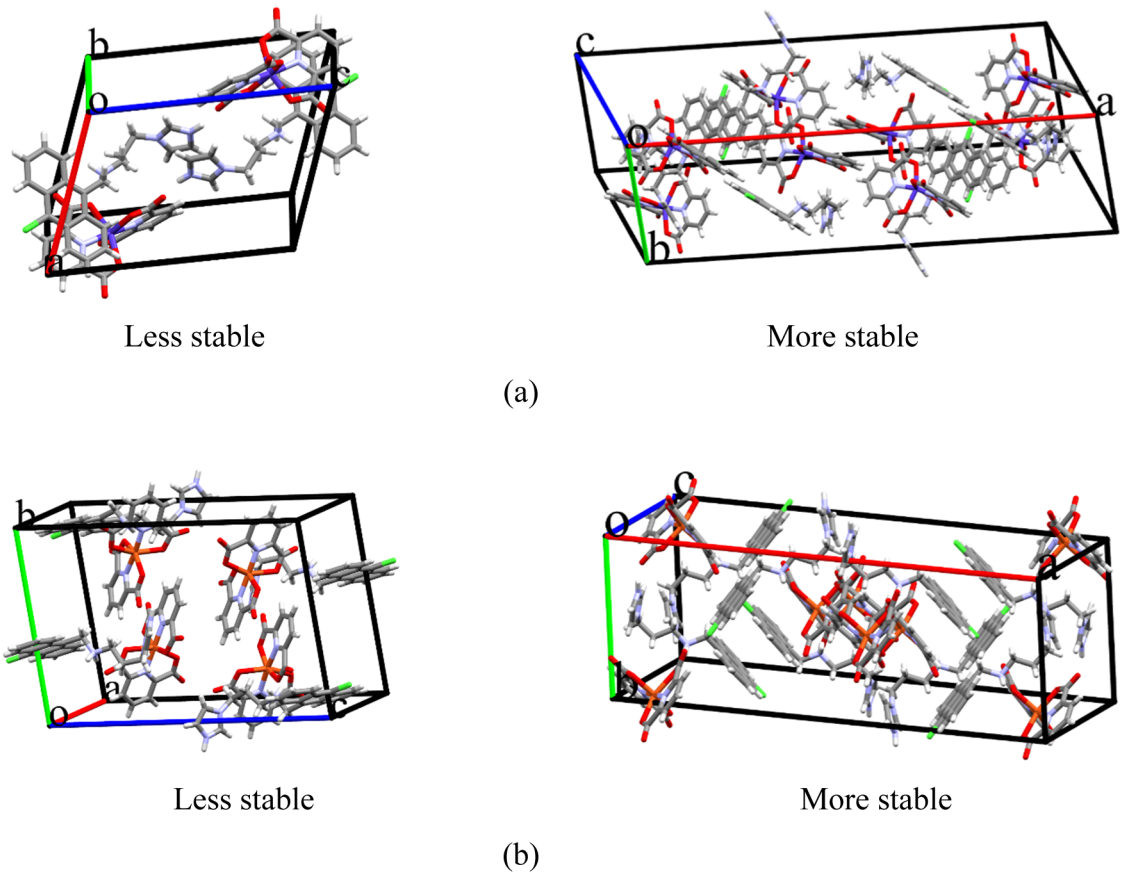

Figure 7. Unit cells of crystals of the hydrates of the (a) cobalt and (b) copper complexes, respectively, that accompany incorporation of water and release of methanol molecule(s) in their formation by crystallization.

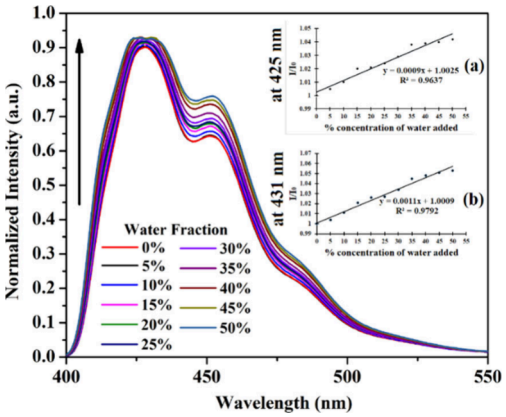

Figure 8. Fluorescence titration of a 2 mL solution taken from a bulk methanol solution containing zinc(II) acetate dihydrate (0.02 mM), $H_2$26pdc (0.04 mM), and **Clanth** (0.02 mM) by adding 0−50% water. Inset (a) and (b): change in fluorescence intensity at 425 and 431 nm after systematic addition of water during titration (excitation at 300 nm).

the zinc complex, there were also two aggregates, but only one could be crystallized. Generally, H or J aggregates of π-stack show distinct emission peaks.[64] Dynamic light scattering study showed that an addition of water to a dilute solution of the reaction mixture of the cobalt complex in methanol initially increased the sizes of particles, which was followed by a decrease in particle sizes (Figure S20). In the case of copper, aggregation was decreased with water addition; hence, upon dilution of the reaction mixture by adding water, the self-assembling in solutions was changed, which was reflected in the assemblies of the crystalline forms.

CONCLUSIONS

The crystals of the stable hydrate of cobalt and copper complexes belonging to monoclinic $C2/c$ space groups were transformed to crystals of a less stable form of hydrates upon dissolution in methanol (triclinic $P\bar{1}$ space group). The transformation from a less stable form to stable form required a bottom up approach. In fact, the crystals of the less stable forms were formed easily as kinetic products, and were dissolved in solvent water, which provided higher amounts of sites and ways for hydrogen bonding; as a result, they were transformed to the stable form of hydrates. In each case, the chloride atoms were away from each other; the C−Cl bonds were projected toward opposite directions, and the nearest neighbors of the chloro-anthracenyl units did not face each other in a head on manner. The stable forms had extensive stacking among the cations to form a zigzag ladder-like structure, which had chelate−chelate stacking and embraced the anions. Under sealed conditions, the less stable form could be stored for several days. The advantage of these crystalline hydrates was that they could be crystallized repeatedly but with change in the crystallite sizes, as illustrated in Figure S21. Thus, controlling concentration is not only the advantage of crystallization, but the effects of water molecules replacing methanol molecules and vice versa contributed to the reversible crystallization. The stable forms of hydrates had

https://doi.org/10.1021/acsomega.4c08822
ACS Omega 2024, 9, 47848−47856

extensive chelated anions at parallel positions suitable for coming close to form stacks; they were stabilized by hydrogen bonds of water and ammonium ion. However, the less stable forms had either stacked dimers or stacked chain of anions, which were dislodged to form stable forms by displacement among them. This provided a new paradigm to study a system that underwent reversibly reconstructive noncovalent assemblies of hydrates.

■ ASSOCIATED CONTENT

Supporting Information

The Supporting Information is available free of charge at https://pubs.acs.org/doi/10.1021/acsomega.4c08822.

The structural diagrams, spectroscopic details, morphology, thermograms, bond parameters of the hydrates (PDF)

The crystallographic information files have the CCDC numbers 2363160−64 and 2385089 (CIF)

■ AUTHOR INFORMATION

Corresponding Author

Jubaraj B. Baruah − *Department of Chemistry, Indian Institute of Technology Guwahati, Guwahati, Assam 781 039, India*; orcid.org/0000-0003-3371-7529; Email: juba@iitg.ac.in

Author

Abhay Pratap Singh − *Department of Chemistry, Indian Institute of Technology Guwahati, Guwahati, Assam 781 039, India*

Complete contact information is available at: https://pubs.acs.org/10.1021/acsomega.4c08822

Author Contributions

A.P.S. contributed as a Ph.D. student under the supervision of J.B.B. and both the authors have contributed equally.

Notes

The authors declare no competing financial interest.

■ ACKNOWLEDGMENTS

The authors thank the Ministry of Education, Government of India, New Delhi, for financial support through a departmental grant (F. O. 5-1/2014-TS. VII), the Department of Chemistry, IIT Guwahati, and Department of Science and Technology, New-Delhi India, for using the SCXRD facility (Sanction No. SR/FST/CS-II/2017/23) provided by them for structure elucidation and various instrument facilities, and the Central Instrumentation facility of IIT Guwahati for general facilities.

■ REFERENCES

(1) *A reversible reaction of hydrated copper(II) sulfate*; Royal Society of Chemistry, 2024. https://edu.rsc.org/experiments/a-reversible-reaction-of-hydrated-copperii-sulfate/437.article.

(2) *The equilibrium between two coloured cobalt species*; Royal Society of Chemistry, 2024. https://edu.rsc.org/experiments/the-equilibrium-between-two-coloured-cobalt-species/1.article.

(3) Wells, A. F. The crystal structures of salt hydrates and complex halides. *Q. Rev. Chem. Soc.* **1954**, *8*, 380−403.

(4) Sanii, R.; Patyk-Kazmierczak, E.; Hua, C.; Darwish, S.; Pham, T.; Forrest, K. A.; Space, B.; Zaworotko, M. J. Toward an understanding of the propensity for crystalline hydrate formation by molecular compounds. Part 2. *Cryst. Growth Des.* **2021**, *21*, 4927−4939.

(5) Li, R.; Shi, Y.; Shi, L.; Alsaedi, M.; Wang, P. Harvesting water from air: using anhydrous salt with sunlight. *Environ. Sci. Technol.* **2018**, *52*, 5398−5406.

(6) Xu, Y.; Wang, Q.; Shen, C.; Lin, Q.; Wang, P.; Lu, M. A series of energetic metal pentazolate hydrates. *Nature* **2017**, *549*, 78−81.

(7) Leung, A. F.; Hayashibara, L.; Spadaro, J. Fluorescence properties of uranyl nitrates. *J. Phys. Chem. Solids* **1999**, *60*, 299−304.

(8) Zhang, Y.; Chen, H.-M.; Lin, M.-J. Chiral self-discrimination induced luminescence vapochromism of binaphthol imides for anti-counterfeiting and data encryption. *Adv. Optical Mater.* **2024**, *12*, 24.

(9) Zhou, F.; Gu, P.; Luo, Z.; Bisoyi, H. K.; Ji, Y.; Li, Y.; Xu, Q.; Li, Q.; Lu, J. Unexpected organic hydrate luminogens in the solid state. *Nature Commun.* **2021**, *12*, 2339.

(10) Kimura, T.; Choppin, G. R. Luminescence study on determination of the hydration number of Cm(III). *J. Alloys Compd.* **1994**, *213-214*, 313−317.

(11) Sagami, T.; Tahara, Y. O.; Miyata, M.; Miyake, H.; Shinoda, S. Luminescence sensing of weakly-hydrated anions in aqueous solution by self-assembled europium(III) complexes. *Chem. Commun.* **2017**, *53*, 3967−3970.

(12) Tarai, A.; Baruah, J. B. Changing π-interactions and conformational adjustments of N-(isonicotinylhydrazide)-1,8-naphthalimide by hydration and complexation affect photophysical properties. *Cryst. Growth Des.* **2018**, *18*, 456−465.

(13) Xin, Y.; Wang, J.; Zychowicz, M.; Zakrzewski, J. J.; Nakabayashi, K.; Sieklucka, B.; Chorazy, S.; Ohkoshi, S.-I. Dehydration-hydration switching of single-molecule magnet behavior and visible photoluminescence in a cyanido-bridged $Dy^{III}Co^{III}$ framework. *J. Am. Chem. Soc.* **2019**, *141*, 18211−18220.

(14) Wu, D.-Q.; Shi, L.; Shao, D.; Xia, M.; Liao, Y.; Wu, Y.; Wen, J.; Zhai, B. Dehydration-actuated single-molecule magnet behavior in a cyanide-bridged $[Fe_2Co_2]$ cluster featuring zigzag structure. *J. Mol. Struct.* **2024**, *1295*, 136615.

(15) Lu, Z.; Wang, X.; Liu, Z.; Liao, F.; Gao, S.; Xiong, R.; Ma, H.; Zhang, D.; Zhu, D. Tuning the magnetic behavior via dehydration/hydration treatment of a new ferrimagnet with the composition of $K_{0.2}Mn_{1.4}Cr(CN)_6{\cdot}6H_2O$. *Inorg. Chem.* **2006**, *45*, 999−1004.

(16) Chen, W.-X.; Gao, Y.-F.; Gao, P.-Y.; Liu, Q.-P.; Zhuang, G.-L. Ionothermal synthesis, magnetic transformation and hydration-dehydration properties of Co(II)-based coordination polymers. *RSC Adv.* **2016**, *6*, 71952−71957.

(17) Skokanova, Z.; Krocan, J.; Rakos, M. Effect of water of crystallization on magnetic properties of $MgSO_4$. *Czech. J. Phys.* **1978**, *28*, 220−227.

(18) Heczko, M.; Nowicka, B. Switching of magnetic properties by topotactic reaction in a 1D CN-bridged Ni(II)−Nb(IV) system. *Dalton Trans.* **2024**, *53*, 5788−5795.

(19) Sadakiyo, M.; Yamada, T.; Kitagawa, H. Hydrated proton-conductive metal-organic frameworks. *ChemplusChem.* **2016**, *81*, 691−701.

(20) Li, Y. M.; Hibino, M.; Miyayania, M.; Kudo, T. Proton conductivity of tungsten trioxide hydrates at intermediate temperature. *Solid State Ionics* **2000**, *134*, 271−279.

(21) Bjorheim, T. S.; Norby, T.; Haugsrud, R. Hydration and proton conductivity in $LaAsO_4$. *J. Mater. Chem.* **2012**, *22*, 1652−1661.

(22) Martinelli, A.; Otero-Mato, M. N.; Garaga, K.; Elamin, S. M. H.; Rahman, J. W.; Zwanziger, U.; Werner-Zwanziger, J. M.; Varela, L. M. A new solid-state proton conductor: the salt hydrate based on imidazolium and 12-tungstophosphate. *J. Am. Chem. Soc.* **2021**, *143*, 13895−13907.

(23) Cha, J.-H.; Shin, K.; Choi, S.; Lee, S.; Lee, H. Maximized proton conductivity of the HPF_6 clathrate hydrate by structural transformation. *J. Phys. Chem. C* **2008**, *112*, 13332−13335.

(24) Maegawa, K.; Wlazło, M.; Phuc, N. H. H.; Hikima, K.; Kawamura, G.; Nagai, A.; Matsuda, A. Synthesis and structure-electrochemical property relationships of hybrid imidazole-based proton conductors for medium-temperature anhydrous fuel cells. *Chem. Mater.* **2023**, *35*, 7708−7718.

(25) Ratcliffe, C. I. The Development of Clathrate Hydrate Science. *Energy Fuels* **2022**, *36*, 10412−10429.
(26) Sloan, E. D., Jr. Fundamental principles and applications of natural gas hydrates. *Nature* **2003**, *426*, 353−363.
(27) Mamontov, E.; Cheng, Y.; Daemen, L. L.; Keum, J. K.; Kolesnikov, A. I.; Pajerowski, D.; Podlesnyak, A.; Ramirez-Cuesta, A. J.; Ryder, M. R.; Stone, M. B. Effect of hydration on the molecular dynamics of hydroxychloroquine sulfate. *ACS Omega* **2020**, *5*, 21231−21240.
(28) Khankari, R. K.; Grant, D. J. W. Pharmaceutical hydrates. *Thermochim. Acta* **1995**, *248*, 61−79.
(29) Gomez, D. T.; Pratt, L. R.; Asthagiri, D. N.; Rempe, S. B. Hydrated anions: from clusters to bulk solution with quasi-chemical theory. *Acc. Chem. Res.* **2022**, *55*, 2201−2212.
(30) Nath, J. K.; Baruah, J. B. Water assisted anion chains and anion dependent fluorescence emission in salts of N,N′-bis(3-imidazol-1-ylpropyl)naphthalenediimide. *New J. Chem.* **2013**, *37*, 1509−1519.
(31) Lopez-Corbalan, V.; Fuertes, A.; Llamas-Saiz, A. L.; Amoriin, M.; Granja, J. R. Recognition of anion-water clusters by peptide-based supramolecular capsules. *Nature Commun.* **2024**, *15*, 6055.
(32) Ryan, M. J.; Gao, L.; Valiyaveetil, F. I.; Kananenka, A. A.; Zanni, M. T. Water inside the selectivity filter of a K^+ ion channel: structural heterogeneity, picosecond dynamics, and hydrogen bonding. *J. Am. Chem. Soc.* **2024**, *146*, 1543−1553.
(33) Mondal, C.; Ganguly, M.; Pal, J.; Sahoo, R.; Sinha, A. K.; Pal, T. Pure inorganic gel: a new host with tremendous sorption capability. *Chem. Commun.* **2013**, *49*, 9428−9430.
(34) Lu, B.; Cheng, H.; Qu, L. Inorganic hydrogel based on low-dimensional nanomaterials. *ACS Nano* **2024**, *18*, 2730−2749.
(35) Krishnan, B. P.; Sureshan, K. M. A spontaneous single-crystal-to-single-crystal polymorphic transition Involving major packing changes. *J. Am. Chem. Soc.* **2015**, *137*, 1692−1696.
(36) Harsha, P.; Khan, M.; Thakuria, R.; Das, D. Synthesis of a cocrystal hydrate by sublimation and reversible polymorphic transformation through single-crystal to single-crystal fashion. *Cryst. Growth Des.* **2024**, *24*, 3109−3113.
(37) Das, D.; Engel, E.; Barbour, L. J. Reversible single-crystal to single-crystal polymorphic phase transformation of an organic crystal. *Chem. Commun.* **2010**, *46*, 1676−1678.
(38) Weissbuch, I.; Torbeev, V. Y.; Leiserowitz, L.; Lahav, M. Solvent effect on crystal polymorphism: why addition of methanol or ethanol to aqueous solutions induces the precipitation of the least stable β form of glycine. *Angew. Chem., Int. Ed.* **2005**, *44*, 3226−3229.
(39) DeMatos, L. L.; Williams, A. C.; Booth, S. W.; Petts, C. R.; Taylor, D. J.; Blagden, N. Solvent influences on metastable polymorph lifetimes: Real-time interconversions using energy dispersive X-Ray diffractometry. *J. Phram. Chem.* **2007**, *96*, 1069−1078.
(40) Blagden, N.; Davey, R. J.; Lieberman, H. F.; Williams, L.; Payne, R.; Roberts, R.; Rowe, R.; Docherty, R. Crystal chemistry and solvent effects in polymorphic systems Sulfathiazole. *J. Chem. Soc., Faraday Trans.* **1998**, *94*, 1035−1044.
(41) Gu, C.-H.; Young, V., Jr.; Grant, D. J. W. Polymorph screening: Influence of solvents on the rate of solvent-mediated polymorphic transformation. *J. Pharm. Sci.* **2001**, *90*, 1878−1890.
(42) Song, Z.; Liu, X.; Yang, C.; Wu, Q.; Guo, X.; Liu, G.; Wei, Y.; Meng, L.; Dang, Y. Methanol-induced crystallization of chiral hybrid manganese (II) chloride single crystals for achieving circularly polarized luminescence and second harmonic generation. *Adv. Optical Mater.* **2024**, *12*, 2301272.
(43) Liu, X.; Beysens, D.; Bourouina, T. Water harvesting from air: current passive approaches and outlook. *ACS Mater. Lett.* **2022**, *4*, 1003−1024.
(44) Lin, Y.-H.; Lin, H.-H.; Lee, Y.-S.; Yu, W.-Y.; Luo, S.-C.; Kang, D.-Y. MOF-303 with lowered water evaporation enthalpy for solar steam generation. *ACS Appl. Mater. Interfaces* **2024**, *16*, 49640−49650.
(45) Braun, D. E.; Karamertzanis, P. G.; Price, S. L. Which, if any, hydrates will crystallise ? Predicting hydrate formation of two dihydroxybenzoic acids. *Chem. Commun.* **2011**, *47*, 5443−5445.
(46) Braun, D. E. Supramolecular organisation of sulphate salt hydrates exemplified with brucine sulphate. *CrystEngComm* **2020**, *22*, 7204−7216.
(47) Braun, D. E.; Gelbrich, T.; Kahlenberg, V.; Griesser, U. J. The eight hydrates of strychnine sulfate. *Cryst. Growth Des.* **2020**, *20*, 6069−6083.
(48) Wu, Y.; Breeze, M. I.; Clarkson, G. J.; Millange, F.; O'Hare, D.; Walton, R. I. Exchange of coordinated solvent during crystallization of a metal-organic framework observed by in situ high-energy X-ray diffraction. *Angew. Chem., Int. Ed.* **2016**, *55*, 4992−4996.
(49) Singh, A. P.; Baruah, J. B. π-Stacking among the anthracenyl groups of a copper complex resulted in doubling of unit cell volume to provide new polymorphs. *ACS Omega* **2023**, *8*, 30776−30787.
(50) Singh, A. P.; Baruah, J. B. Hydrates of N-(anthracen-9-ylmethyl)-3-(1H-imidazolium-1-yl)propan-1-ammonium zinc(II) or cobalt(II) 2,6-pyridinedicarboxylate: inter-conversions, assembling and utilities. *Inorg. Chem. Commun.* **2024**, *168*, 112883.
(51) Jing, Y.; Zhang, J.; Wan, M.; Xue, J.; Liu, J.; Qin, J.; Hong, Z.; Du, Y. Distinguishing polymorphs of ethenzamide-saccharin cocrystal based on terahertz and Raman vibrational spectroscopic techniques. *IEEE Trans. Terahertz Sci. and Technol.* **2024**, *14*, 152−161.
(52) Chen, T.; Li, M.; Liu, J. $\pi-\pi$ Stacking interaction: a nondestructive and facile means in material engineering for bio applications. *Cryst. Growth Des.* **2018**, *18*, 2765−2783.
(53) Moulton, B.; Zaworotko, M. J. From molecules to crystal engineering: supramolecular isomerism and polymorphism in network solids. *Chem. Rev.* **2001**, *101*, 1629−1658.
(54) Zhang, L.; Kuhling, F.; Mattsson, A.-M.; Lisanne Knijff, L.; Hou, X.; Ek, G.; Dufils, T.; Gjorup, F. H.; Kantor, I.; Zhang, C.; Brant, W. R.; Edström, K.; Berg, E. J. Reversible hydration enabling high-rate aqueous Li-ion batteries. *ACS Energy Lett.* **2024**, *9*, 959−966.
(55) Leguy, A. M. A; Hu, Y.; Campoy-Quiles, M.; Alonso, M. I.; Weber, O. J.; Azarhoosh, P.; van Schilfgaarde, M.; Weller, M. T.; Bein, T.; Nelson, J.; Docampo, P.; Barnes, P. R. F. Reversible hydration of $CH_3NH_3PbI_3$ in films, single crystals, and solar cells. *Chem. Mater.* **2015**, *27*, 3397−3407.
(56) Yang, Z.; Zeng, Q.; Zhou, X.; Zhang, Q.; Nie, F.; Huang, H.; Li, H. Cocrystal explosive hydrate of a powerful explosive, HNIW, with enhanced safety. *RSC Adv.* **2014**, *4*, 65121−65126.
(57) Pandith, A.; Kumar, A.; Kim, H.-S. 9-*N*-Alkylaminomethylanthracene probes for selective fluorescence sensing of pentafluorophenol. *RSC Adv.* **2015**, *5*, 81808−81816.
(58) Singh, A. P.; Baruah, J. B. Arrangements of fluorophores in the salts of imidazole tethered anthracene derivatives with pyridinedicarboxylic acids influencing photoluminescence. *Materials Adv.* **2022**, *3*, 3513−3525.
(59) Sredojevic, D. N.; Tomic, Z. D.; Zaric, S. D. Evidence of chelate-chelate stacking interactions in crystal structures of transition-metal complexes. *Cryst. Growth Des.* **2010**, *10*, 3901−3908.
(60) Ninkovic, D. B.; Janjic, G. V.; Zaric, S. D. Crystallographic and ab initio study of pyridine stacking interactions. local nature of hydrogen bond effect in stacking interactions. *Cryst. Growth Des.* **2012**, *12*, 1060−1063.
(61) Kapteijn, G. M.; Grove, D. M.; van Koten, G.; Smeets, W. J. J.; Spek, A. L. A new mixed alkoxo aryloxo palladium complex with a bidentate nitrogen donor system. *Inorg. Chim. Acta* **1993**, *207*, 131−134.
(62) Meusburger, J. M.; Ende, M.; Talla, D.; Wildner, M.; Miletich, R. Transformation mechanism of the pressure-induced C2/c to P1 transition in ferrous sulfate monohydrate single crystals. *J. Solid State Chem.* **2019**, *277*, 240−252.
(63) Mączka, M.; Sobczak, S.; Krys, M.; Leite, F. F.; Paraguassu, W.; Katrusiak, A. Mechanism of pressure-induced phase transitions and structure-property relations in methylhydrazinium manganese hypophosphite perovskites. *J. Phys. Chem. C* **2021**, *125*, 10121−10129.
(64) Ma, S.; Du, S.; Pan, G.; Dai, S.; Xu, B.; Tian, W. Organic molecular aggregates: from aggregation structure to emission property. *Aggregate* **2021**, *2*, No. e96.

https://doi.org/10.1021/acsomega.4c08822
ACS Omega 2024, 9, 47848−47856